***Supporting Information***

# Ultralow-Iridium content NiIr Alloy Derivative Nanochain Arrays as Bifunctional Electrocatalysts for Overall Water Splitting

*Zhengyang Cai,[ab] Ping Wang,[*b] Xianglong Zhao,[c] Xiuming Bu,[b] Jiajia Zhang,[b] Yuhao Chen,[ab] Jingcheng Xu,[a] Ya Yan,[b] Aiying Chen[*a] and Xianying Wang[*b]*

[a] School of Materials and Chemistry, University of Shanghai for Science and Technology, 200093, Shanghai, P. R. China. E-mail: aychen@usst.edu.cn

[b] Energy Materials Research Center Institute of Ceramics, Chinese Academy of Sciences, 200050, Shanghai, P. R. China. E-mail: wangping@mail.sic.ac.cn, wangxianying@mail.sic.ac.cn

[c] School of Science, Shandong Jianzhu University, Jinan, 250101, P. R. China.

## Figures and Tables

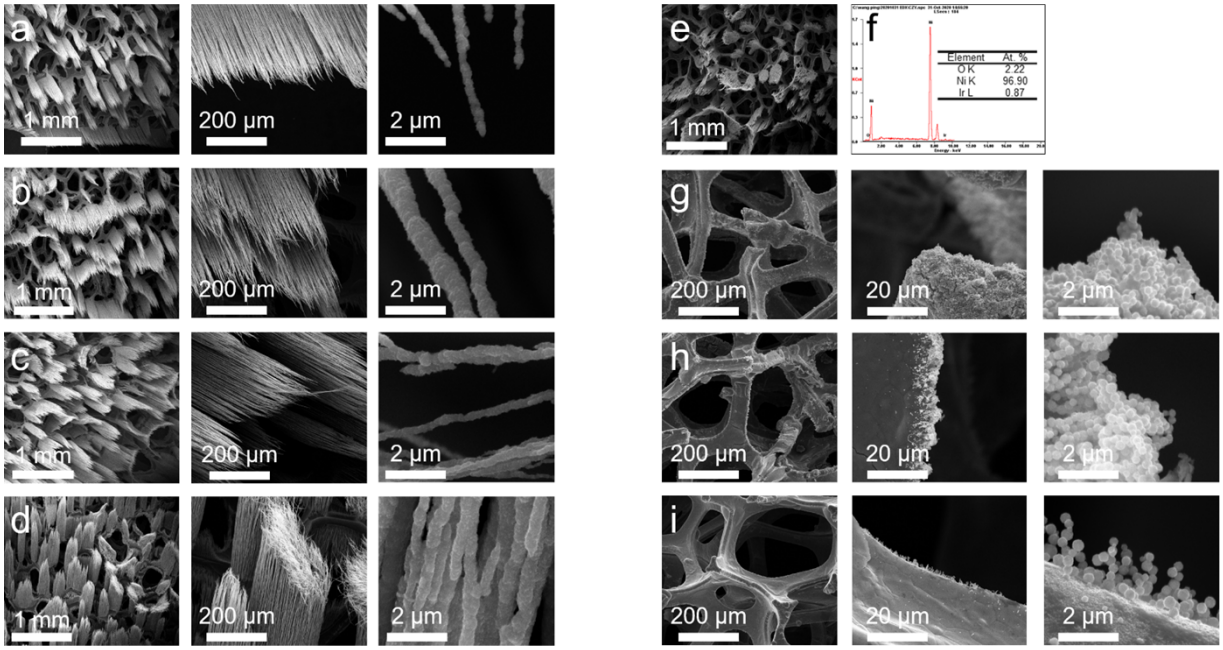


Fig. S1 SEM images of $NiIr_x$ NCs from low to high magnifications. (a) $NiIr_{0.01}$ NCs, (b) $NiIr_{0.1}$ NCs, (c) $NiIr_{0.5}$ NCs, (d) $NiIr_{0.9}$ NCs, (e) $NiIr_1$ NCs, (f) EDX results of Ir, Ni and O in $NiIr_1$ NCs. Inset table is the corresponding atomic ratio, (g) $NiIr_5$ NCs, (h) $NiIr_{10}$ NCs, (i) $NiIr_{20}$ NCs.

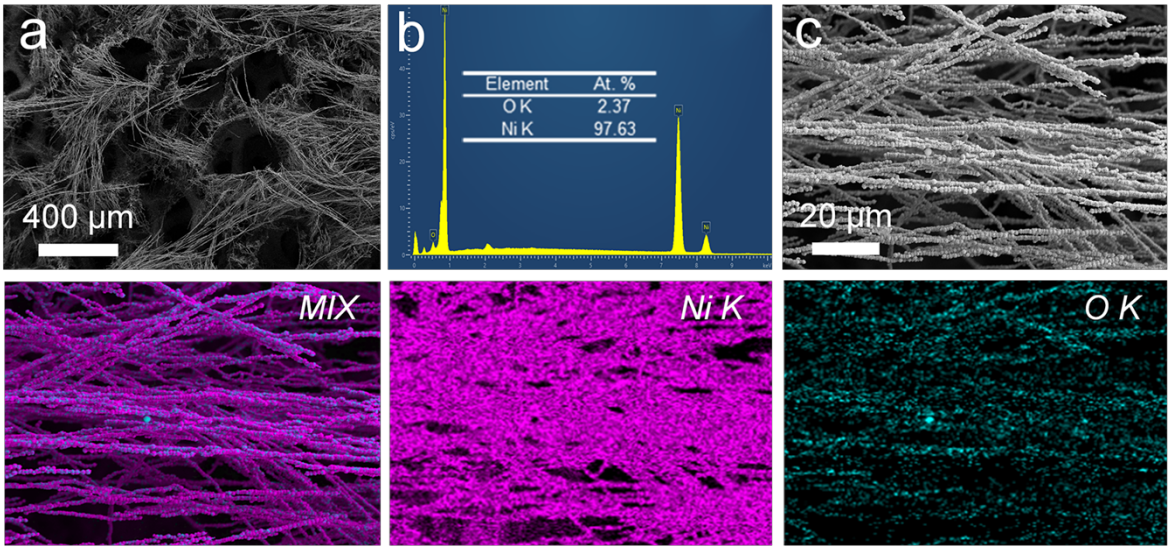


Fig. S2 SEM-EDX analysis of $NiIr_0$ NCs. (a) SEM image. (b and c) EDX and elemental mapping results of Ni and O in $NiIr_0$ NCs. Inset table is the corresponding atomic ratio.

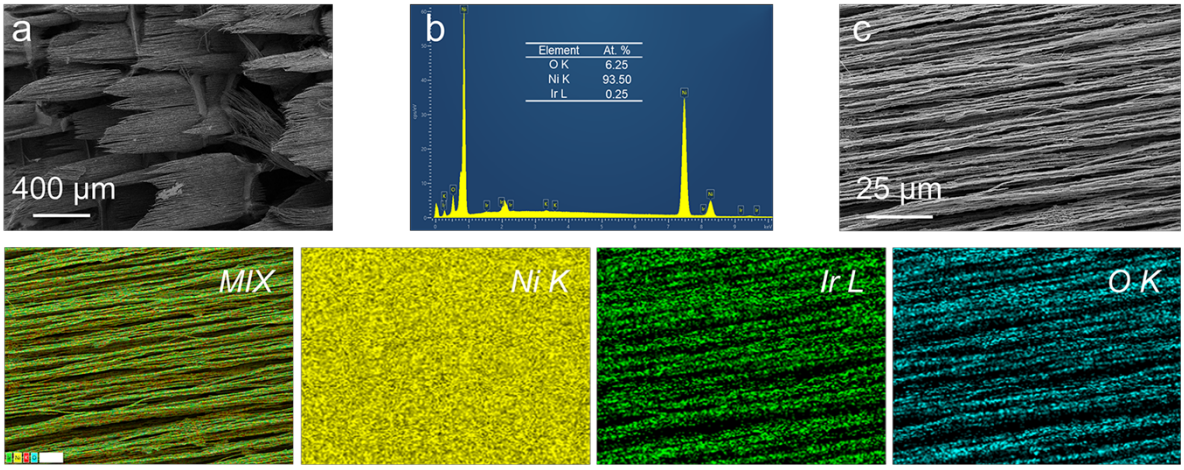


Fig. S3 SEM-EDX analysis of $NiIr_1$ NCs serves as anode after 100 h OER process. (a) SEM image. (b and c) EDX and elemental mapping results of Ir, Ni and O in $NiIr_1$ NCs. Inset table in b is the corresponding atomic ratio.

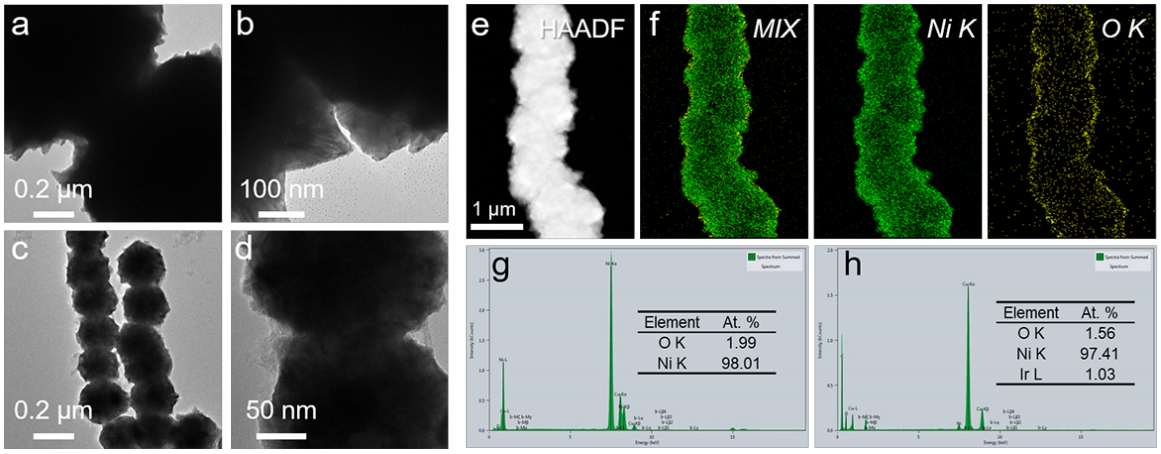


Fig. S4 TEM-EDX analysis of $NiIr_0$ NCs and $NiIr_1$ NCs. (a) TEM image and (b) Position for selected area electron diffraction (SAED) analysis of $NiIr_0$ NCs. (c) TEM image and (d) Position for SAED analysis of $NiIr_1$ NCs. (e) HAADF-STEM image of $NiIr_0$ NCs (f) Corresponding elemental mapping of Ir, Ni and O. EDX result of $NiIr_0$ NCs (g) and $NiIr_1$ NCs (h). The inset tables correspond to their atomic ratio.

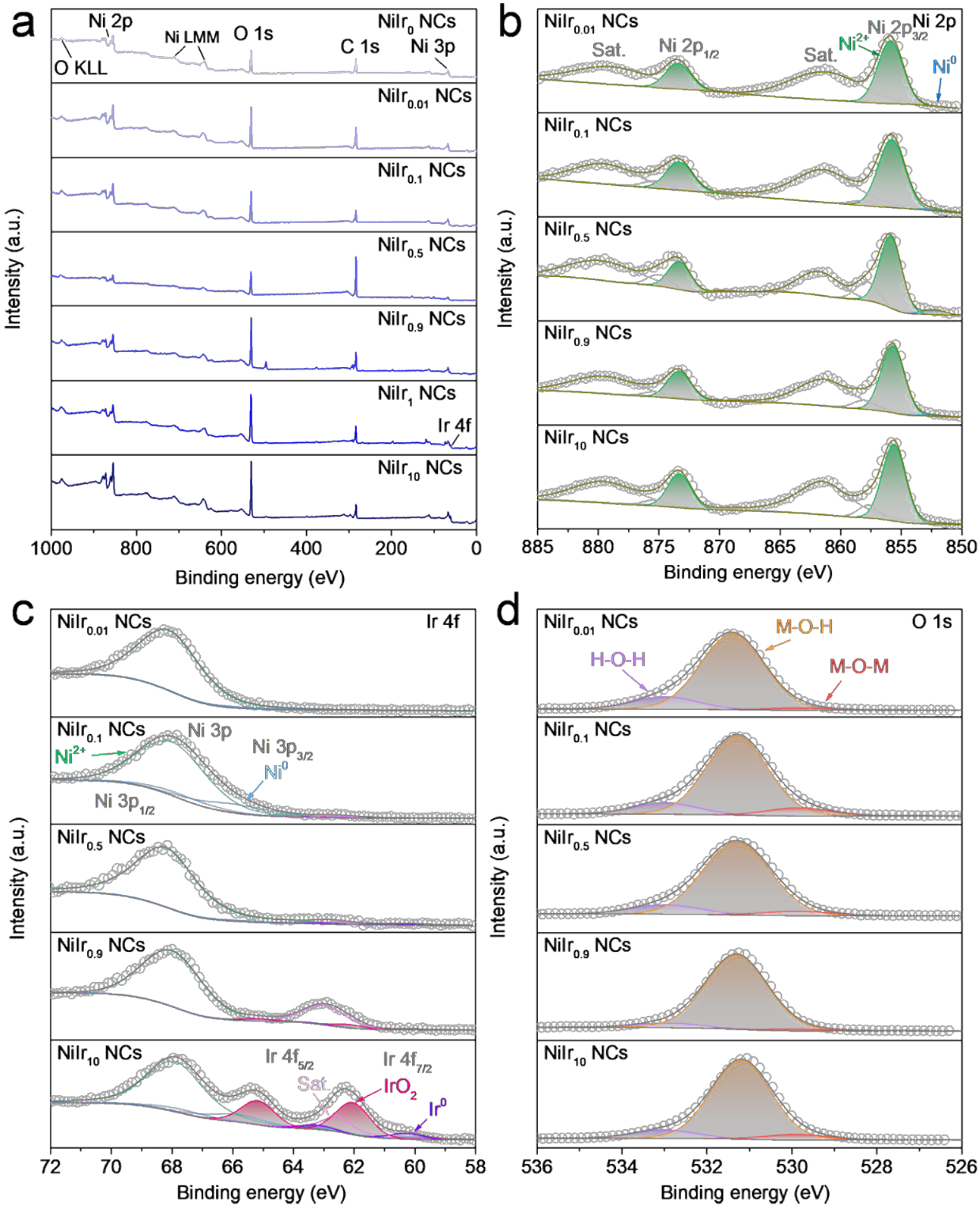


Fig. S5 (a) XPS survey. High-resolution XPS spectra of Ni 2p (b) Ir 4f (c) and O 1s (d) of $NiIr_x$ NCs, x = 0.01, 0.1, 0.5, 0.9, 10.

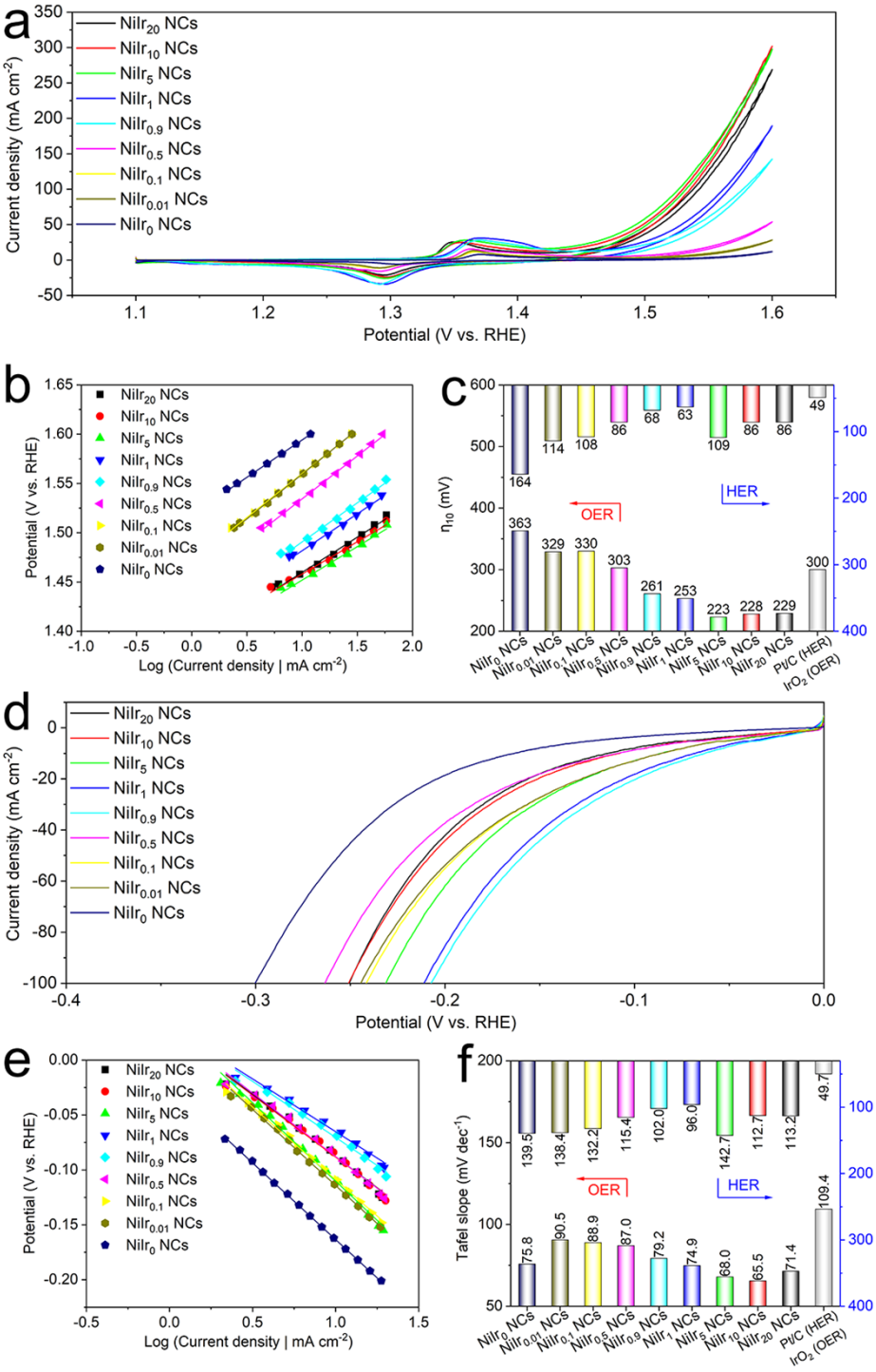


Fig. S6 Electrochemical characterization of $NiIr_x$ NCs (x = 0, 0.01, 0.1, 0.5, 0.9, 1, 5, 10, 20) in 1 M KOH electrolyte. (a) OER CV curves at a scan rate of 5 $mV \cdot s^{-1}$. (b) Tafel plots derived from a. (c) Overpotentials achieved at the current density of 10 $mA \cdot cm^{-2}$ for OER and HER. (d) HER LSV curves at a scan rate of 5 $mV \cdot s^{-1}$. (e) Tafel plots derived from d. (f) Tafel slope values of OER and HER.

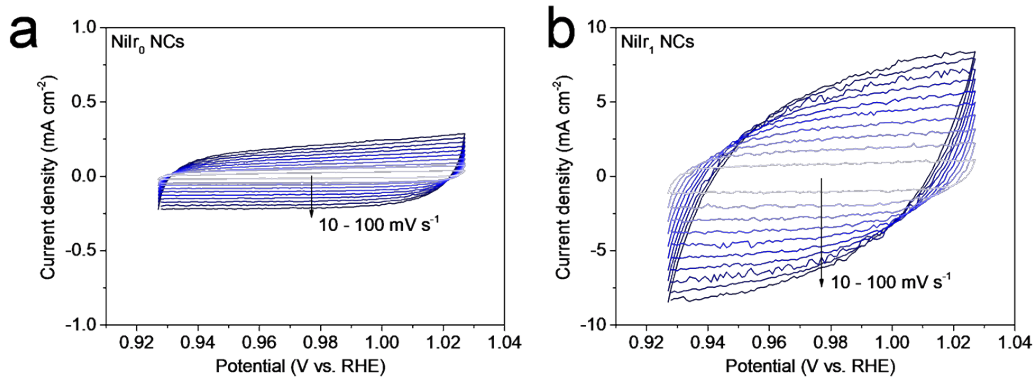


Fig. S7 Cyclic voltammograms measured at different scan rates ranging from 10 to 100 mV·s$^{-1}$. (a) $NiIr_0$ NCs, (b) $NiIr_1$ NCs.

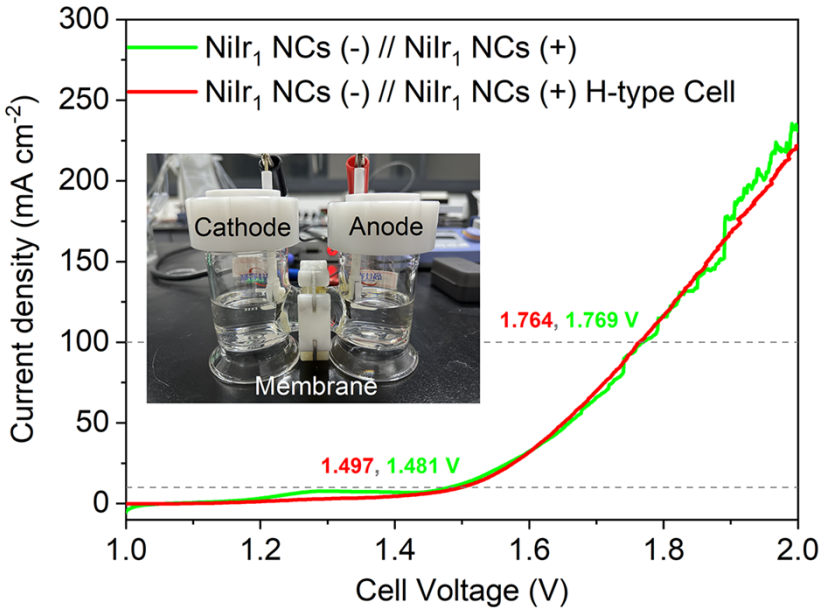


Fig. S8 OWS LSV curves of the $NiIr_1$ NCs // $NiIr_1$ NCs electrode pair in normal cell and H-type cell at a scan rate of 5 mV·s$^{-1}$.

Table S1. Binding energy positions, peak areas and atomic ratio of Ir of $NiIr_x$ NCs, x = 0, 0.01, 0.1, 0.5, 0.9, 1, 10.

| Species | Spectral lines | Peak binding energy (eV) | Peak area | | | | | | |
|---|---|---|---|---|---|---|---|---|---|
| | | | $NiIr_0$ NCs | $NiIr_{0.01}$ NCs | $NiIr_{0.1}$ NCs | $NiIr_{0.5}$ NCs | $NiIr_{0.9}$ NCs | $NiIr_1$ NCs | $NiIr_{10}$ NCs |
| Ni | $2p_{3/2}$ | 852.30 | 21248.89 | 0.00 | 1369.73 | 2345.16 | 1795.58 | 13420.36 | 799.33 |
| $Ni(OH)_2$ | $2p_{3/2}$ | 855.61 | 74362.46 | 108334.50 | 97554.96 | 35932.61 | 92365.72 | 93545.09 | 158810.50 |
| Ni | $2p_{3/2}$, sat | 858.00 | 10505.52 | 0.00 | 6929.57 | 9409.70 | 12181.52 | 6362.47 | 23605.61 |
| $Ni(OH)_2$ | $2p_{3/2}$, sat | 861.23 | 57359.50 | 138641.50 | 130012.90 | 22371.64 | 95498.34 | 70669.76 | 200683.10 |
| Ni | $2p_{1/2}$ | 870.02 | 3384.63 | 0.00 | 526.82 | 586.29 | 426.20 | 2028.25 | 150.82 |
| $Ni(OH)_2$ | $2p_{1/2}$ | 873.32 | 29744.98 | 44390.11 | 40711.95 | 14040.05 | 37980.64 | 38820.38 | 69834.70 |
| Ni | $2p_{1/2}$, sat | 875.30 | 7856.08 | 0.00 | 10234.41 | 5792.76 | 7065.48 | 3168.68 | 12246.09 |
| $Ni(OH)_2$ | $2p_{1/2}$, sat | 879.33 | 44449.87 | 94315.38 | 67845.87 | 30757.27 | 68947.95 | 52450.97 | 134820.70 |
| Ni | $3p_{3/2}$ | 65.94 | 12975.51 | 701.48 | 3676.77 | 245.89 | 214.44 | 10553.30 | 4747.03 |
| Ni | $3p_{1/2}$ | 67.67 | 6487.75 | 350.74 | 1838.38 | 112.34 | 111.51 | 5487.72 | 2373.51 |
| $Ni(OH)_2$ | 3p | 68.00 | 15589.31 | 27809.65 | 22892.06 | 15634.07 | 20393.40 | 15682.48 | 32442.61 |
| Ir | $4f_{7/2}$ | 60.21 | 0.00 | 0.00 | 65.52 | 188.22 | 145.59 | 1908.72 | 1914.57 |
| $IrO_2$ | $4f_{7/2}$ | 62.00 | 0.00 | 0.00 | 43.23 | 12.21 | 594.58 | 5785.56 | 10751.84 |
| $IrO_2$ | $4f_{7/2}$, sat | 62.78 | 0.00 | 0.00 | 416.97 | 364.58 | 5754.92 | 604.95 | 6600.59 |
| Ir | $4f_{5/2}$ | 63.24 | 0.00 | 0.00 | 49.14 | 141.17 | 109.19 | 1431.54 | 1435.92 |
| $IrO_2$ | $4f_{5/2}$ | 65.12 | 0.00 | 0.00 | 32.42 | 9.16 | 445.93 | 4339.17 | 8063.88 |
| H-O-H | | 532.98 | 12538.47 | 25729.79 | 17875.52 | 11748.41 | 11650.00 | 36202.11 | 22860.65 |
| M-O-H | 1s | 531.30 | 90277.04 | 160443.00 | 122459.80 | 94341.52 | 195961.50 | 200270.50 | 210984.40 |
| M-O | | 529.75 | 11579.37 | 5008.66 | 12234.65 | 5698.27 | 4883.99 | 16287.26 | 14681.62 |
| Ir ratio (At. %) | | | 0.00 | 0.00 | 0.02 | 0.02 | 0.19 | 0.38 | 0.75 |

Table S2. OER and HER performance comparison with recently reported noble-metal-based electrocatalysts in 1 M KOH electrolyte.

| Catalysts | Nano structure | Loading ($mg \cdot cm^{-2}$) | $C_{dl}$ ($mF \cdot cm^{-2}$) | OER $\eta_{10}$ (mV) | HER $\eta_{10}$ (mV) | OER Durability (h @ $mA \cdot cm^{-2}$) | Ref. |
|---|---|---|---|---|---|---|---|
| $NiIr_1$ NCs | Nanochains | 1.5 (0.05 Ir) | 59.8 | 253 | 63 | 100 @ 200 | The work |
| 20% Pt/C | Nanoparticles | 1.32 | / | / | 20.1 ± 0.8 | / | 1 |
| AgNi-5 | Nanoparticles | 1.32 | 3.8 | / | 24.0 ± 1.2 | / | |
| $NiPt_3$@NiS | Nanoparticles | 1 | 71 | / | 12 | / | 2 |
| $Rh_3Cu_1$ | Nanotubes | 0.05 | 26 | 315 | 8 | 10 @ 12 | 3 |
| Pt-Cu@$Cu_xO$ | Nanowires | 7.7 | 4.1 | 250 | 72 | 10 @ 20 | 4 |
| NiFePt | Nanocubes | 0.05 | / | 463 | 333 | ~1 @ 12 | 5 |
| NiIr-MOF/NF | Nanosheets | 1 | 5.5 | 350 ($\eta_{100}$) | 17 | / | 6 |
| NiIr@N-C/NF | Nanoparticles | 0.8 | 15.63 | 329 ($\eta_{50}$) | 32 | 10 @ 50 | 7 |
| $NiIr_x$/CNT/CFP | Nanoparticles | 0.09 Ir | 78 | 220 | / | 4 @ 50 | 8 |

Table S3. The Ni and Ir dissolved contents in the electrolyte after 100 h OWS stability test.

| | Ni | Ir |
|---|---|---|
| Content (ppb) | 58.3 | 1.6 |

## Reference

1. R. Majee, A. Kumar, T. Das, S. Chakraborty and S. Bhattacharyya, *Angew. Chem. Int. Ed.*,

2020, **59**, 2881-2889.

2. C. Panda, P. W. Menezes, S. Yao, J. Schmidt, C. Walter, J. N. Hausmann and M. Driess, *J. Am. Chem. Soc.*, 2019, **141**, 13306-13310.
3. D. Cao, H. Xu and D. Cheng, *Adv. Energy Mater.*, 2020, **10**, 1903038.
4. D. T. Tran, H. T. Le, T. L. Luyen Doan, N. H. Kim and J. H. Lee, *Nano Energy*, 2019, **59**, 216-228.
5. M. Fu, Q. Zhang, Y. Sun, G. Ning, X. Fan, H. Wang, H. Lu, Y. Zhang and H. Wang, *Int. J. Hydrogen Energy*, 2020, **45**, 20832-20842.
6. Y. Xu, M. Liu, M. Wang, T. Ren, K. Ren, Z. Wang, X. Li, L. Wang and H. Wang, *Appl. Catal., B*, 2022, **300**, 120753.
7. Y. Xu, X. Chai, M. Liu, T. Ren, S. Yu, Z. Wang, X. Li, L. Wang and H. Wang, *Chem-Eur. J.*, 2020, **26**, 14496-14501.
8. Y. Qiao, Y. Pan, S. Du, T. Wu, Y. Cao, G. Long, W. Fan and F. Zhang, *J. Phys. Chem. C* 2021, **125**, 26003-26012.